Electronic Supplementary Material (ESI) for CrystEngComm.

Supplementary information

3-(4-Methylthiophenyl)acetylacetone – Ups and Downs of Flexibility in the Synthesis of Mixed Metal-Organic Frameworks. Ditopic Bridging of Hard and Soft Cations and Site-Specific Desolvation

Hans Gildenast,[a] Stephanie Nölke,[a] and Ulli Englert*[a,b]

[a] *RWTH Aachen University, Institute of Inorganic Chemistry, Landoltweg 1, 52074, Aachen, Germany. Fax: +49 241 8092288; Tel: +49 241 8094666; E-mail: ullrich.englert@ac.rwth-aachen.de*
[b] *Key Laboratory of Materials for Energy Conversion and Storage, Institute of Molecular Science, Shanxi University, Taiyuan, Shanxi 030006, People's Republic of China*

Contents

S1 Refinement and Crystal Structure Details

Intensity data were collected with a Bruker D8 goniometer equipped with an APEX CCD area detector and an Incoatec microsource (Mo-K_α radiation, $\lambda = 0.71073$ Å, multilayer optics) at 100(2) K (Oxford Cryostream 700 instrument, Oxfordshire, UK). Data were integrated with SAINT[1] and corrected for absorption by multi-scan methods;[2] for this purpose, redundancies between 5 and 12 were achieved. The structures were solved by intrinsic phasing[3] and refined by full matrix least squares procedures based on F^2, as implemented in SHELXL-13.[3] Hydrogen atoms were treated as riding with C−H = 0.98 Å for CH_3 groups, C−H = 0.95 Å for aryl-hydrogen and C−H = 1.00 Å for alkyl-hydrogen bonds. Their isotropic displacement parameters were constrained to U_{iso}(H) = 1.5 U_{eq}(C) for methyl groups or U_{iso}(H) = 1.2 U_{eq}(C) otherwise. The position of OH hydrogen atoms were refined freely.

S1.1 4

The position of the hydroxyl hydrogen atom H2A was refined freely. An ORTEP plot of the crystal structure is shown below.

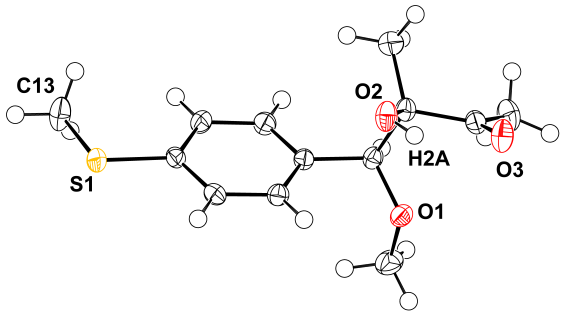

Fig. S1 ORTEP plot of **4** drawn at 70% probability.

S1.2 5

The position of the hydroxyl hydrogen atom H2 was refined freely.

S1.3 6a, 6b and 6c

A satisfactory structure model was obtained for **6a**; the CIF has been deposited with the CCDC and is available electronically. The isotypic solids **6b** and **6c** are affected by additional disorder (see below) and only described for comparison.

No structure model based on geometrically reasonable local density maxima could be derived for the co-crystallized disordered solvent molecules around the $\bar{4}$ inversion axis in **6**. For **6a** SQUEEZE[4] identified solvent accessible voids with a total volume of 216 Å^3 and a content of 52 electrons and was used to correct the low-order reflections for the solvent contribution.

Although **6a-c** are isotypic (Fig. S2), additional disorder in **6b** and **6c** precludes refinement of the well-ordered structure model even for the non-solvent part. In these structures the cavity around the $\bar{4}$ inversion axis does not only contain solvent molecules but also one of the three ligands, namely the one incorporating S3, is disordered with the minority conformer tilted towards the cavity with low site occupancies (7.8(3)% for **6b**, 10.4(3)% for **6c**). This conformation would imply prohibitively short

intermolecular contacts to symmetry equivalent molecules and can therefore only be adopted by one molecule in the vicinity of the $\bar{4}$ site (Fig. S2), with the others necessarily in majority conformation. As the remaining cavity is still filled with solvent molecules and the two aspects of disorder are co-operative, no satisfactory correction with the SQUEEZE algorithm can be achieved. Both approaches neglecting one of these two closely associated aspects of disorder either in the framework or the solvent part do not meet our requirements for a convincing structure model.

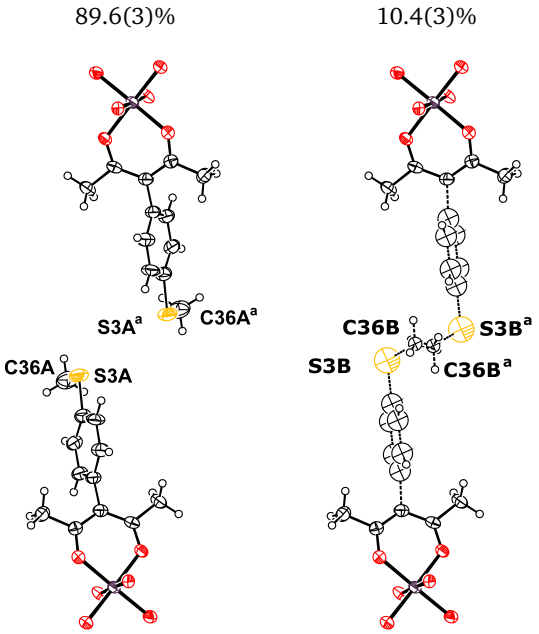

	6a	**6b**	**6c**
a,b / Å	17.703(4)	17.8027(13)	17.826(3)
c / Å	46.013(8)	46.166(3)	45.877(8)
V / Å^3	14420(7)	14632(2)	14578(6)

Fig. S2 (left) ORTEP plots of an excerpt of the crystal structure of **6c** drawn at 50% probability showing the two possible conformations of one of the ligand molecules. d(C36B−C36Ba) = 0.75(4) Å. (right) Table listing the lattice parameters of **6a**, **6b** and **6c**. Symmetry operator: $a = 2-x,\ 1/2-y,\ z$.

S1.4 7c, 7d and 7e

A satisfactory structure model was derived for **7e**; the CIF has been deposited with the CCDC and is available electronically. The isotypic solids **7c** and **7d** are only described for comparison.

Fig. S3 depicts the disorder that occurs in the structure type **7**. **7c** and **7d** were treated by assigning split positions **A** and **B** to the atoms associated with methyl group C12 and to two alternative orientations **A** and **B** for the acetone molecule associated with O13. Only homonymous orientations subtend reasonable intermolecular contacts: the disorder was therefore treated as coupled, with site occupancies in matching orientations constrained to the same value and the sum of the occupancies constrained to unity.

7e on the other hand exhibits a more complex disorder involving a second acetone molecule. In **7e** the acacSMe ligands associated with S2 and S6 exhibit additional disorder and were thus assigned split positions **B** and **B'**. The disorder model was restricted to the PhSMe moieties, as the difference between the alternative orientations of the acetylacetone moieties is too small to be modeled. To retain reasonable intermolecular contacts the occupancy of the additional acetone molecule associated with O14 has to be treated as coupled to the split position **B'** of the PhSMe moieties; these occupancies were therefore constrained to the same value (Fig. S3). Furthermore the acetone molecule associated with O14 is only compatible with the **B** orientation of C12. This disorder was, however, not directly treated

as coupled using constraints, as it is still chemically sound as long as the occupancy of the acetone associated with O14 is lower than the site occupancy of C12B.

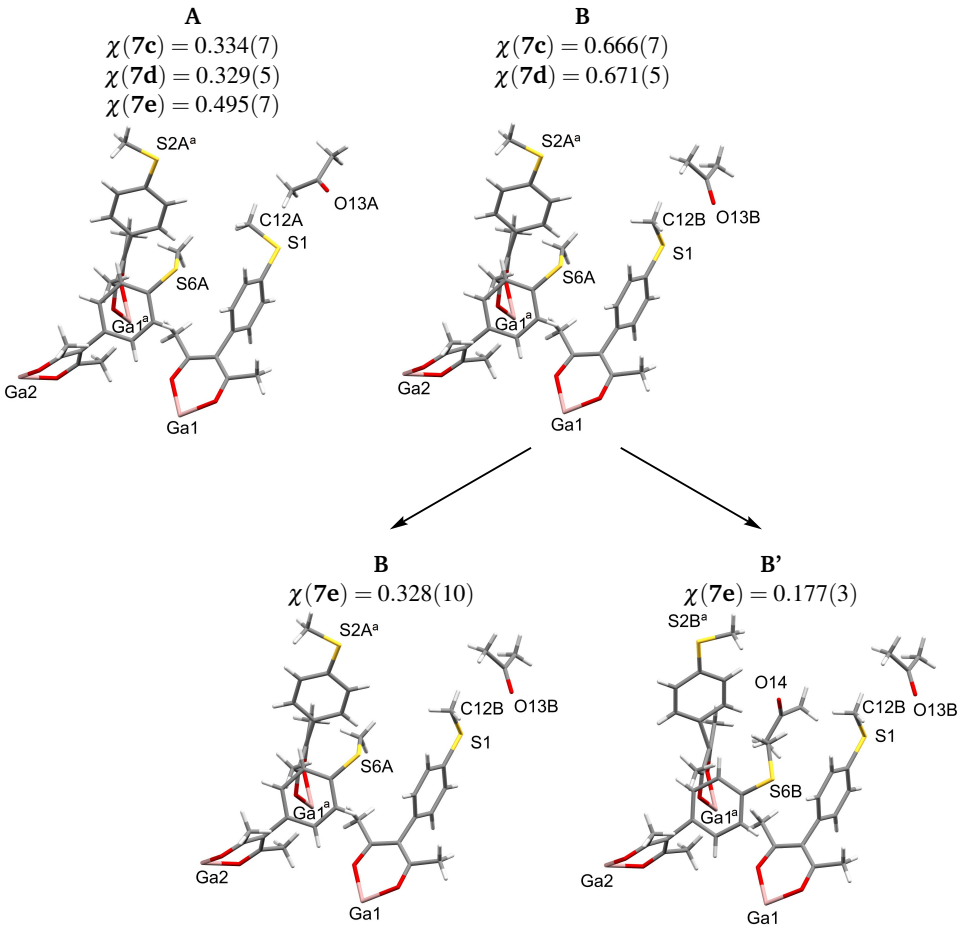

Fig. S3 Cooperative disorder in **7e**. The three alternative orientations are depicted in picture **A**, **B** and **C** with their respective occupancy χ. Symmetry operator: $a = 1-x,\ 1-y,\ 1-z$.

Despite the different disorder patterns the three compounds essentially have the same unit cell (Tab. S1).

Table S1 Lattice parameters of **7c-e**.

	7c	**7d**	**7e**
a / Å	14.589(4)	14.6243(9)	14.603(4)
b / Å	25.540(7)	25.7787(15)	25.521(7)
c / Å	20.309(6)	20.1194(12)	20.434(6)
β / Å	100.318(4)	100.652(2)	100.830(4)
V / Å^3	7445(4)	7454.2(8)	7480(4)

Even a restrained model for the co-crystallized acetone molecules remained unsatisfactory. They were assigned the geometry of a published crystal structure[5] and treated as rigid fragments in the refinement, with a common isotropic displacement parameter for all non-hydrogen atoms in all acetone residues.

S1.5 8a

The structure contains considerable residual electron density that suggests a disorder for the acac-SMePh ligand associated with S1. Tentative refinement of a disordered model resulted in a low occupancy of ca. 0.1 for the minority conformer and led to convergence problems; this more complicated model was therefore discarded.

S1.6 Thermal removal of $CHCl_3$ from 8c

In order to investigate the partial removal of a $CHCl_3$ molecule from **8c**, a single crystal was fixed with two-component adhesive to a glass fiber. Diffraction data were collected at 100 K with intervening heating cycles at 360 K. During these cycles the crystal was heated to 320 K with a ramp of 360 K h^{-1} and subsequently to 360 K at 120 K h^{-1}. The temperature of 360 K was then kept for 15 min, followed by fast cooling to 100 K. For each data set thus obtained the diffraction data were integrated to the same threshold of 0.83 Åand the refinement was conducted with the same number of variables. For the last two data sets not all non-hydrogen atoms could be assigned acceptable anisotropic displacement parameters. Occupancy refinement of **CLF2** was conducted with fixed displacement parameters taken from the data collection on the pristine crystal prior to the first heating cycle.

S1.7 8f

The occupancy of the alternative trivalent cations Al1 and Ga1 sharing the same site was refined while fractional coordinates and displacement parameters were constrained to be equal and the sum of the site occupancies was constrained to unity. Systematic data truncation had been suggested as a tool to judge the reliability of such refined occupancies.[6] In addition to our refinement with all data, test refinements excluding 20% of the reflections with (I) the lowest resolution and (II) the highest resolution were conducted. Tab. S2 shows that the refined occupancies do not vary significantly.

Table S2 Occupation of Ga1 in **8f** in dependance of data truncation.

	(I)	(II)	(III)
resolution of excluded reflections	> 1.25 Å	< 0.79 Å	-
number of unique reflections	9825	9825	12305
occupation of Ga1	0.450(9)	0.447(3)	0.447(3)

Table S3 Coordination sphere of **8b**, **8e** and **8f** in comparison. Listed are the mean $M^{III}-O$ bond lengths $\bar{d}$ and the mean square root of the difference of the ADP component in the direction of the respective bond $\sqrt{\Delta_{ADP}}$.

	8b	**8e**	**8f**
$\bar{d}(M^{III}-O)$ / Å	1.878(9)	1.944(12)	1.910(15)
$\sqrt{\Delta_{ADP}}$ ($M^{III}-O$) / Å	0.032(13)	0.031(13)	0.056(8)
$\sqrt{\Delta_{ADP}}$ (C−O) / Å	0.048(14)	0.004(3)	0.058(16)

S2 Structure type 8 data

Table S4 Comparison of the different parameters for **8a** - **8f** mentioned in the main text. Symmetry operators: $a = x-1,\ y,\ z$; $b = 1-x,\ 1-y,\ 1-z$. *bpr*: progress along the berry pseudorotation axis.

parameters	**8a**	**8b**	**8c**	**8d**	**8e**	**8f**
d(Ag1−O9)	2.646(2)	2.649(2)	2.6566(5)	2.664(6)	2.644(3)	2.649(2)
d(Ag1−O10^a)	2.797(2)	2.776(3)	2.7782(5)	2.764(6)	2.777(4)	2.791(2)
bpr(Ag1) / %	50.9	51.6	52.6	55.4	52.5	51.7
τ(Ag1)	0.52	0.52	0.50	0.47	0.51	0.51
Cl3···Cl3^b / Å	3.2968(14)	3.2978(14)	3.319(2)	3.331(3)	3.294(2)	3.3008(12)
C37−Cl3···Cl3^b / °	153.48(11)	153.13(13)	154.50(16)	154.1(3)	153.84(17)	153.66(11)
V(**CLF1** void) / Å^3	125	123	127	129	126	121
V(**CLF2** void) / Å^3	145	145	142	155	143	146

S3 Powder Patterns

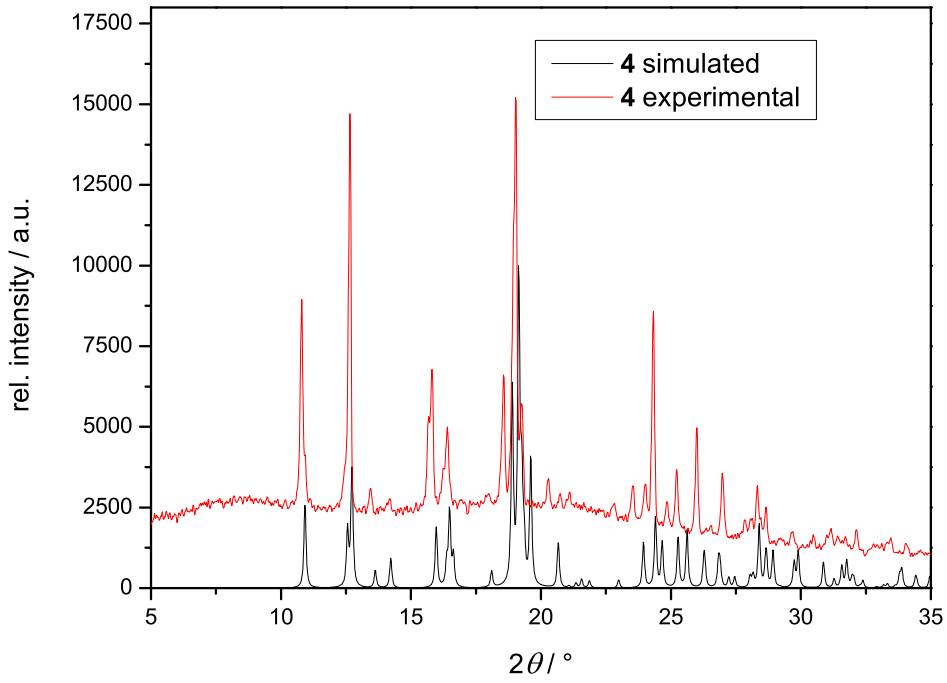

Fig. S4 Simulated and experimental powder pattern of **4**.

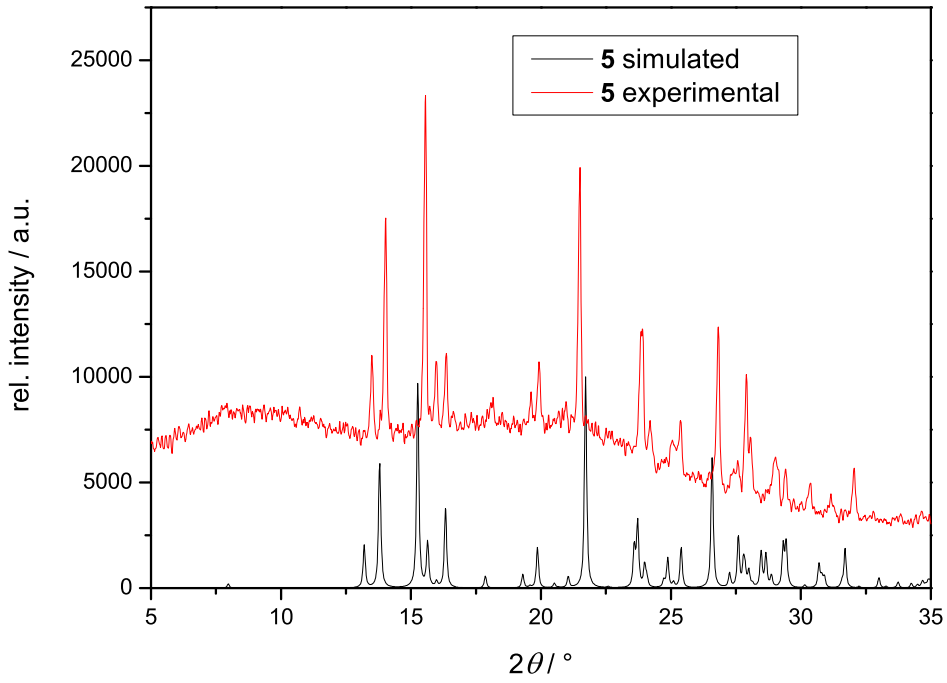

Fig. S5 Simulated and experimental powder pattern of **5**.

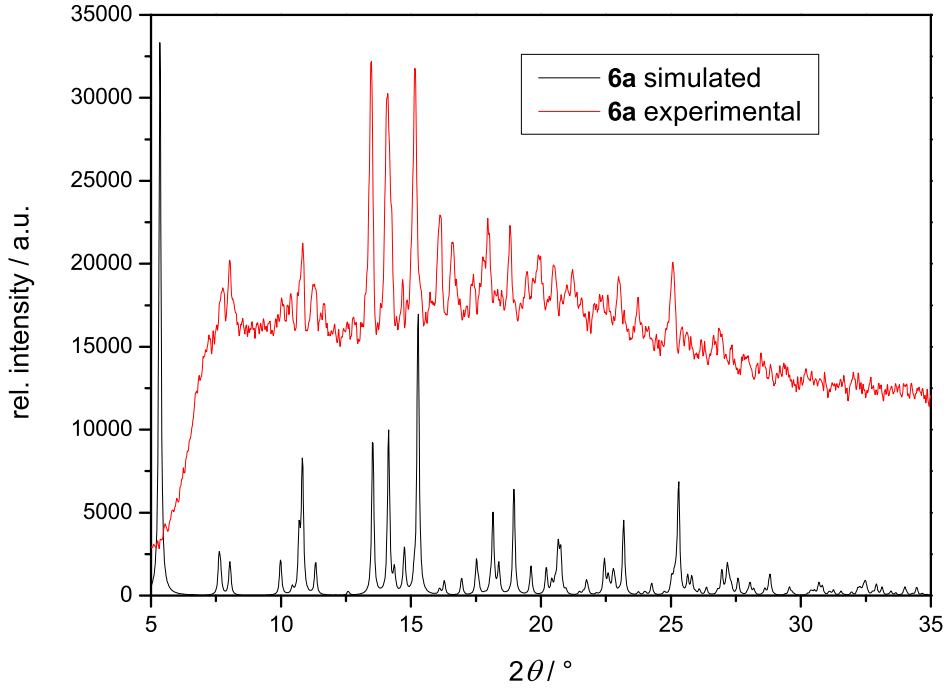

Fig. S6 Simulated and experimental powder pattern of **6a**.

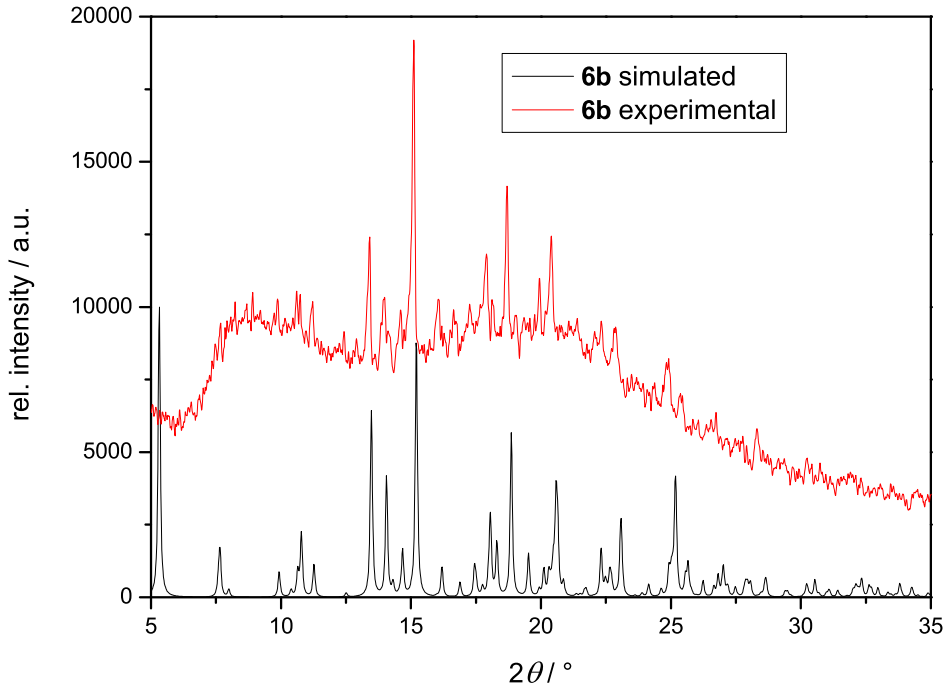

Fig. S7 Simulated and experimental powder pattern of **6b**.

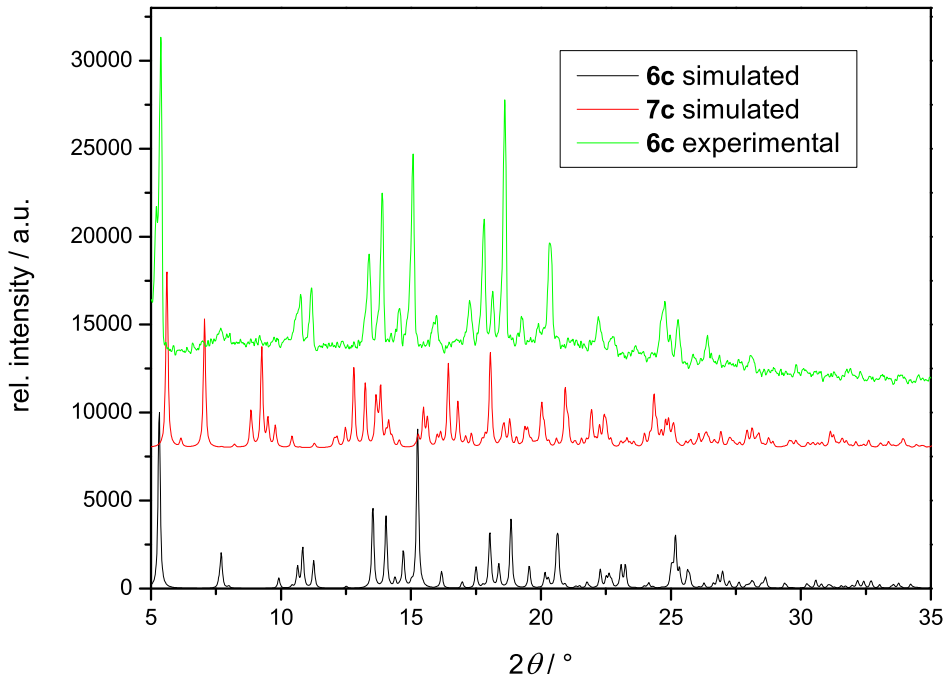

Fig. S8 Simulated powder pattern of **7c** and simulated and experimental powder pattern of **6c**. For this compound **6c** is the dominant crystal structure that represents the bulk material. No experimental powder pattern matching **7c** could be recorded.

For the Fe^{III} complex **7d** no matching powder pattern could be recorded.

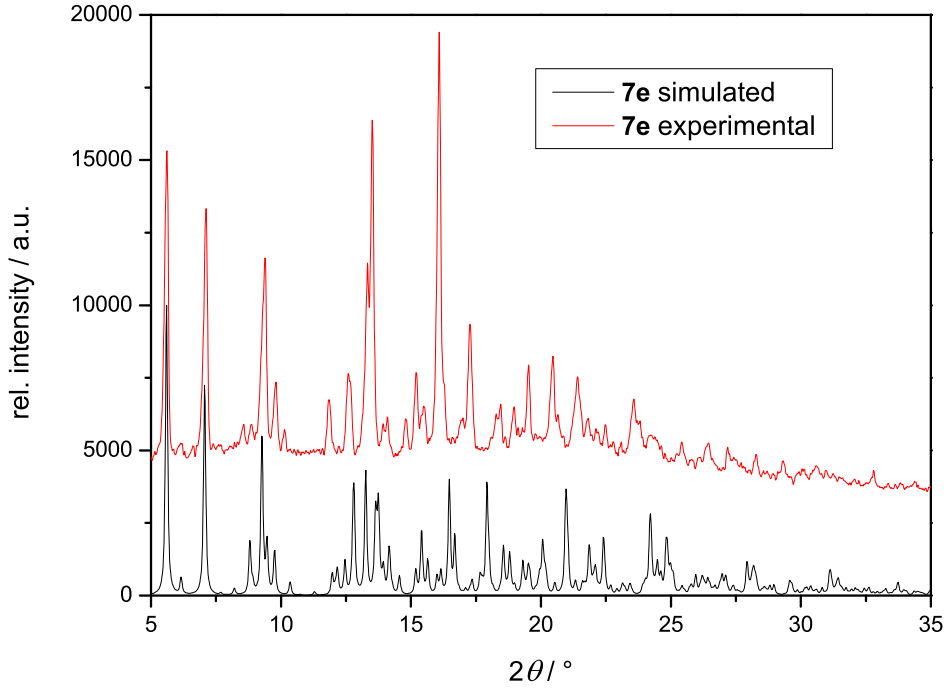

Fig. S9 Simulated and experimental powder pattern of **7e**.

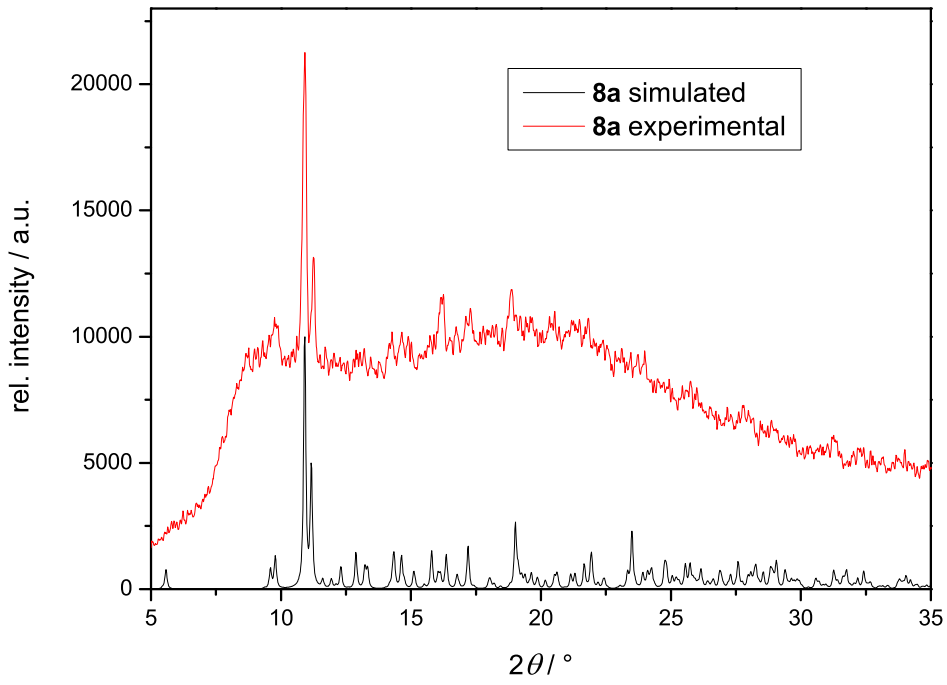

Fig. S10 Simulated and experimental powder pattern of **8a**.

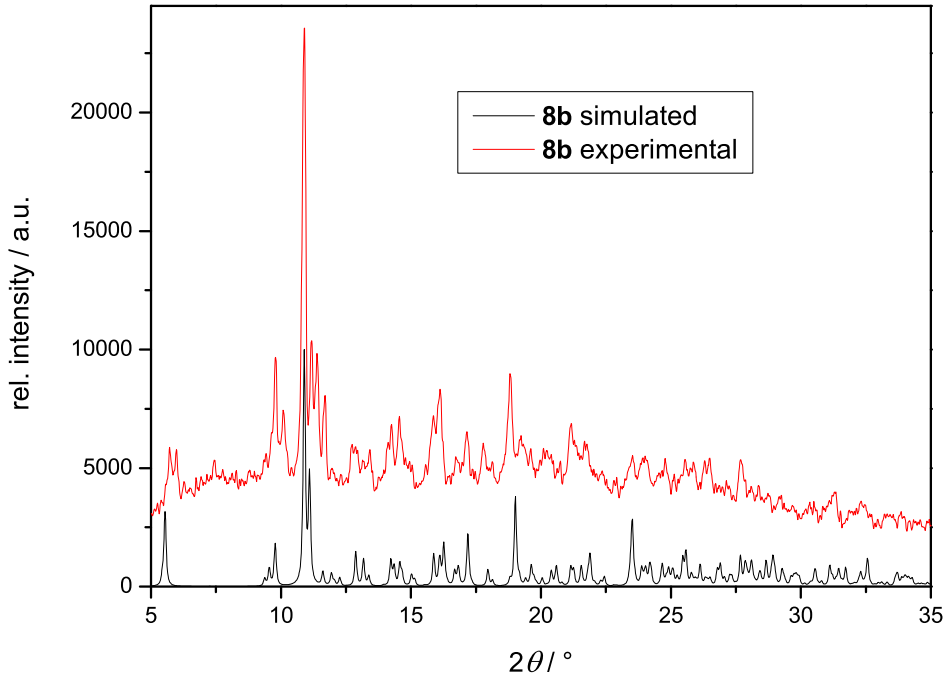

Fig. S11 Simulated and experimental powder pattern of **8b**.

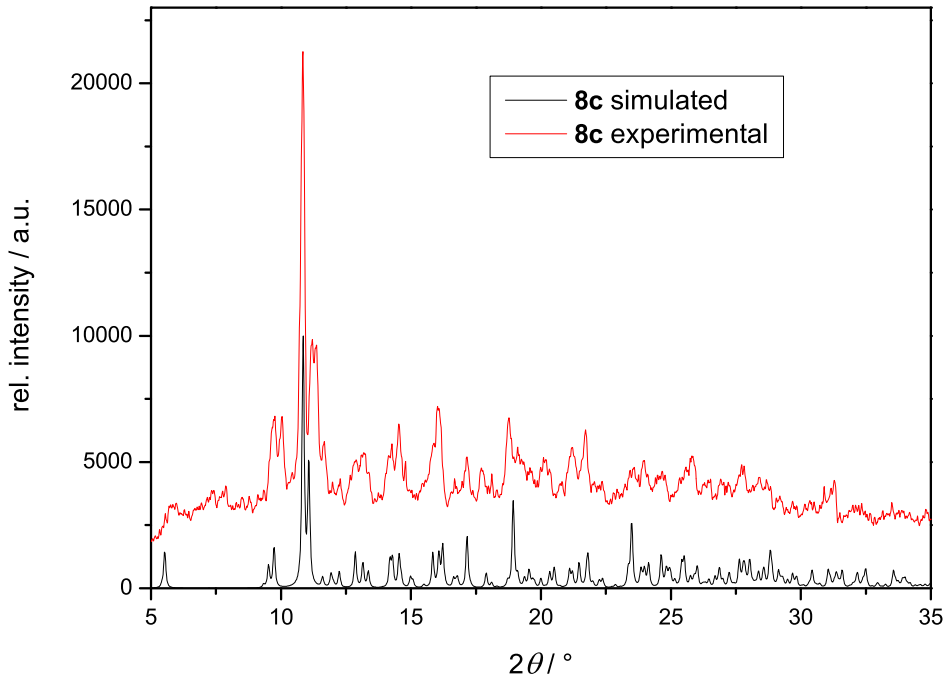

Fig. S12 Simulated and experimental powder pattern of **8c**.

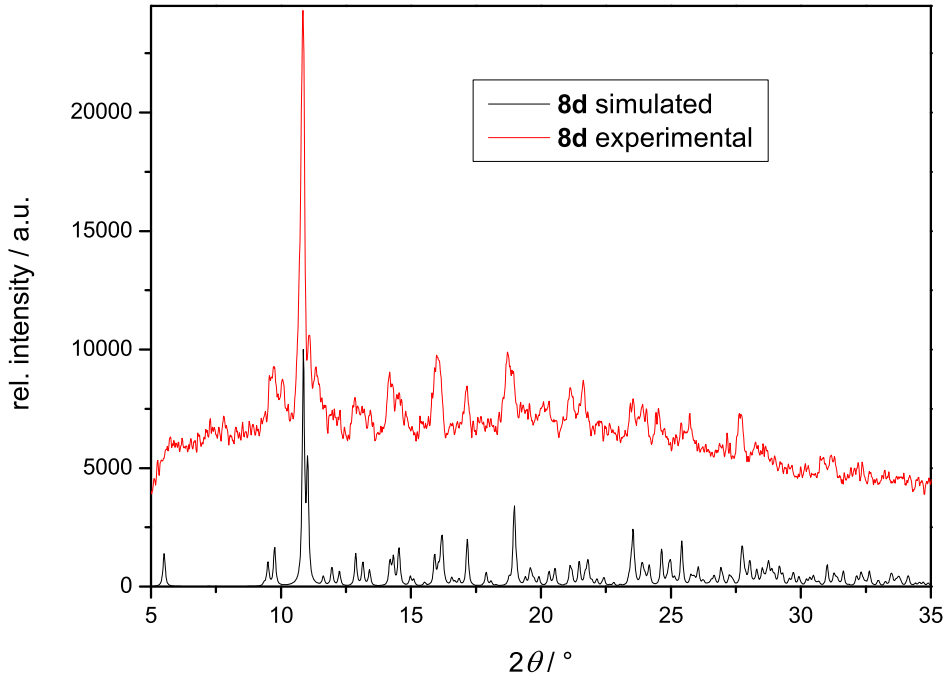

Fig. S13 Simulated and experimental powder pattern of **8d**.

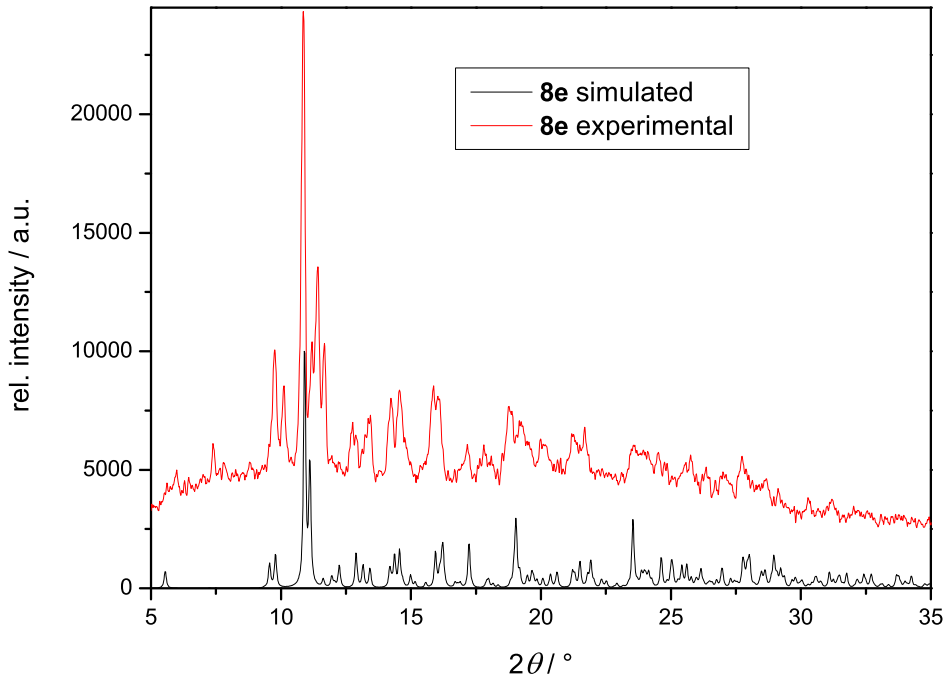

Fig. S14 Simulated and experimental powder pattern of **8e**.

S4 NMR spectra

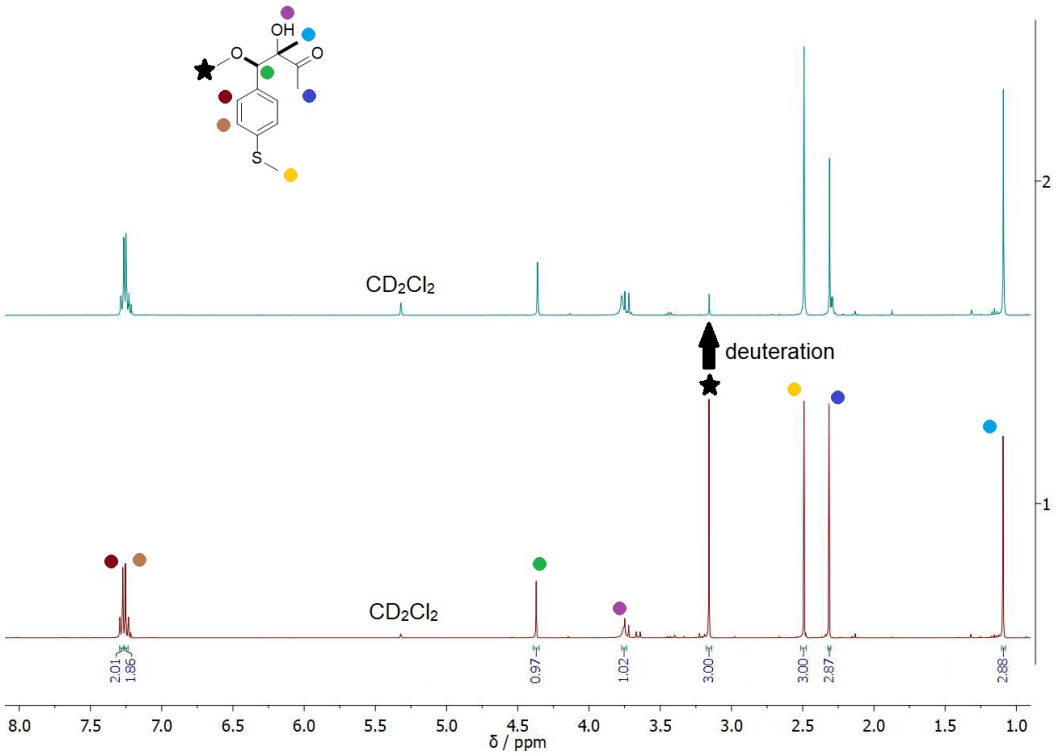

Fig. S15 ^{1}H-NMR spectra of **4** (bottom) and **4**-d_3 (top). Measured in CD_2Cl_2 at 298 K and 400 MHz.

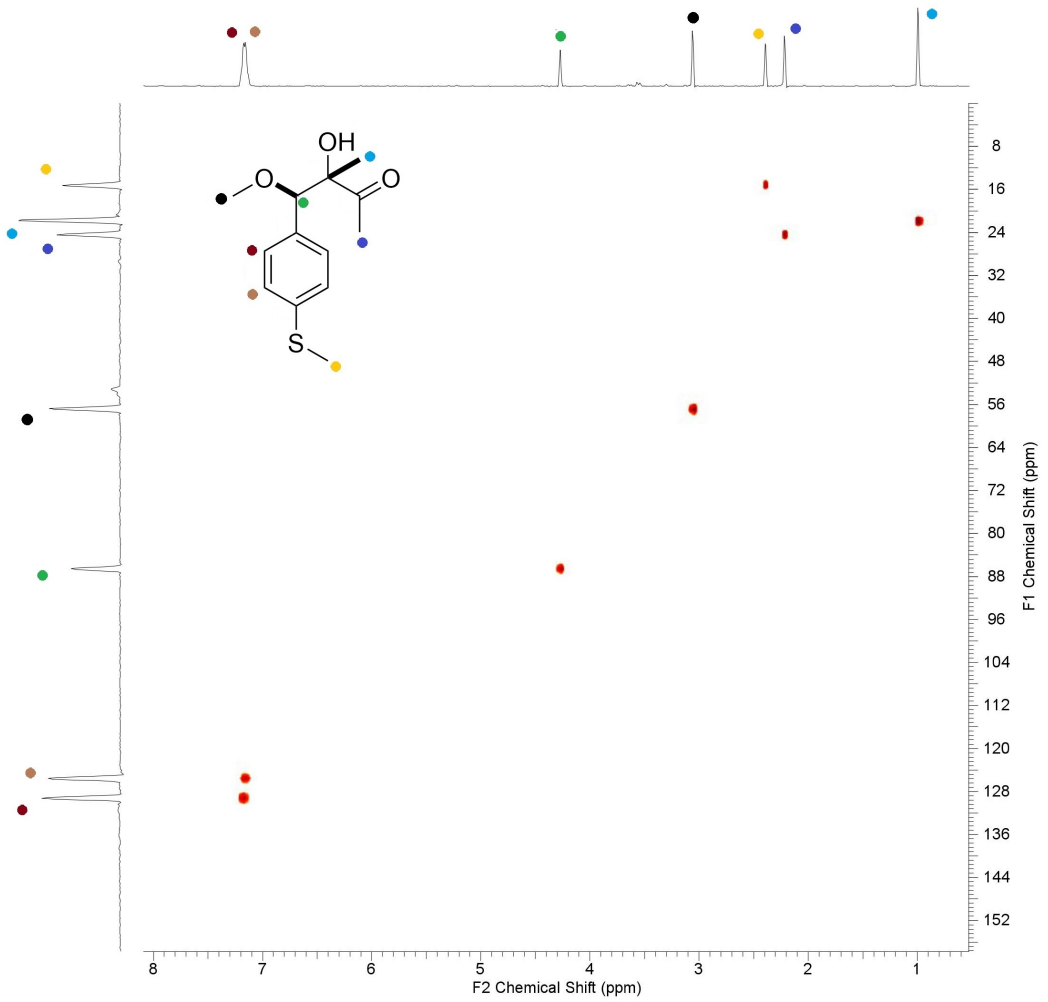

Fig. S16 HSQC spectrum of **4**. Measured in CD_2Cl_2 at 298 K.

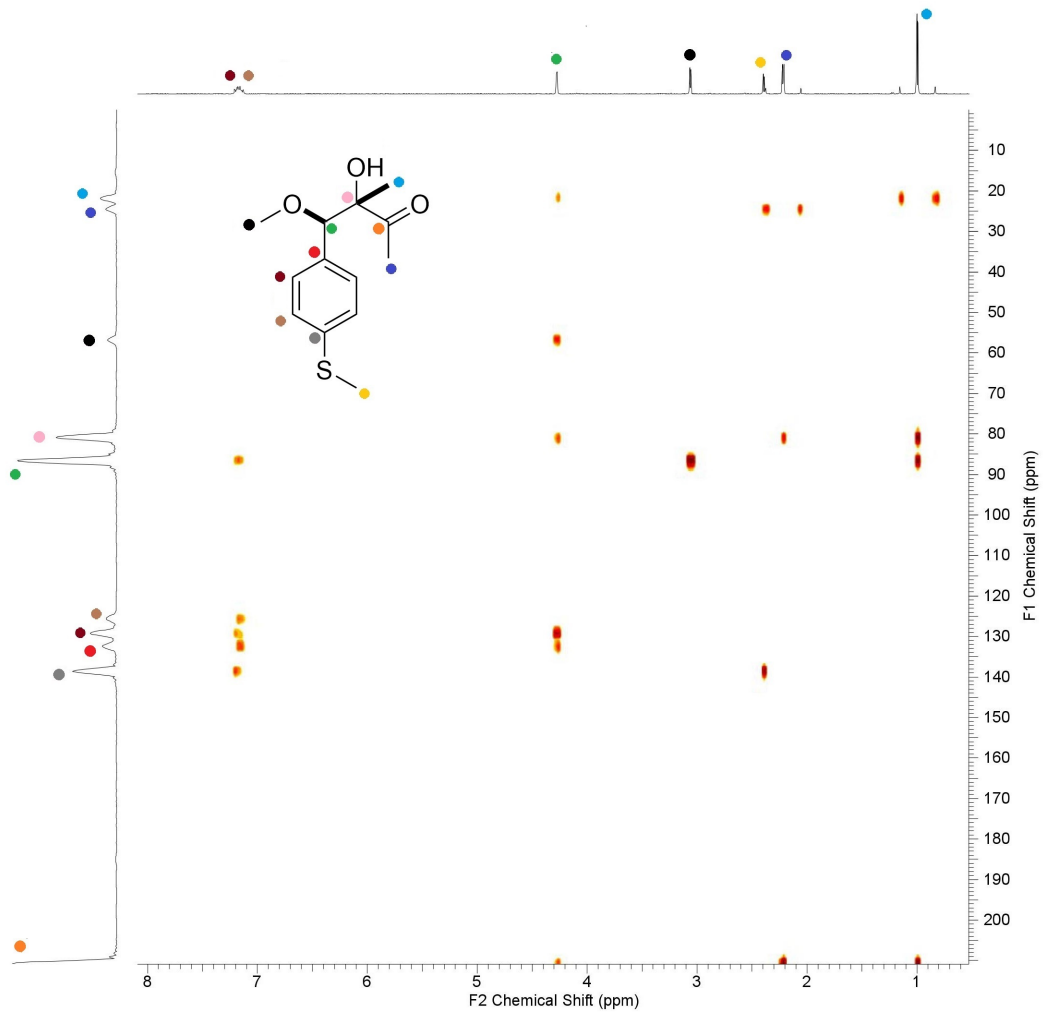

Fig. S17 HMBC spectrum of **4**. Measured in CD_2Cl_2 at 298 K.

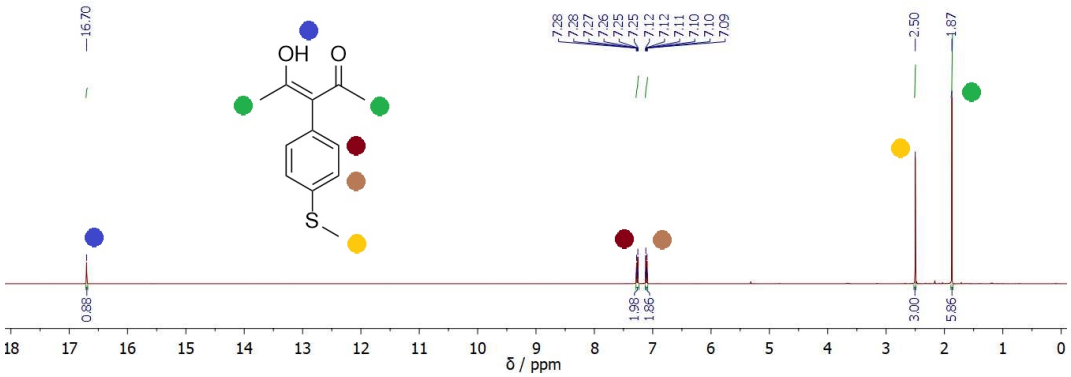

Fig. S18 ^{1}H-NMR spectrum of **5**. Measured in CD_2Cl_2 at 298 K and 400 MHz.

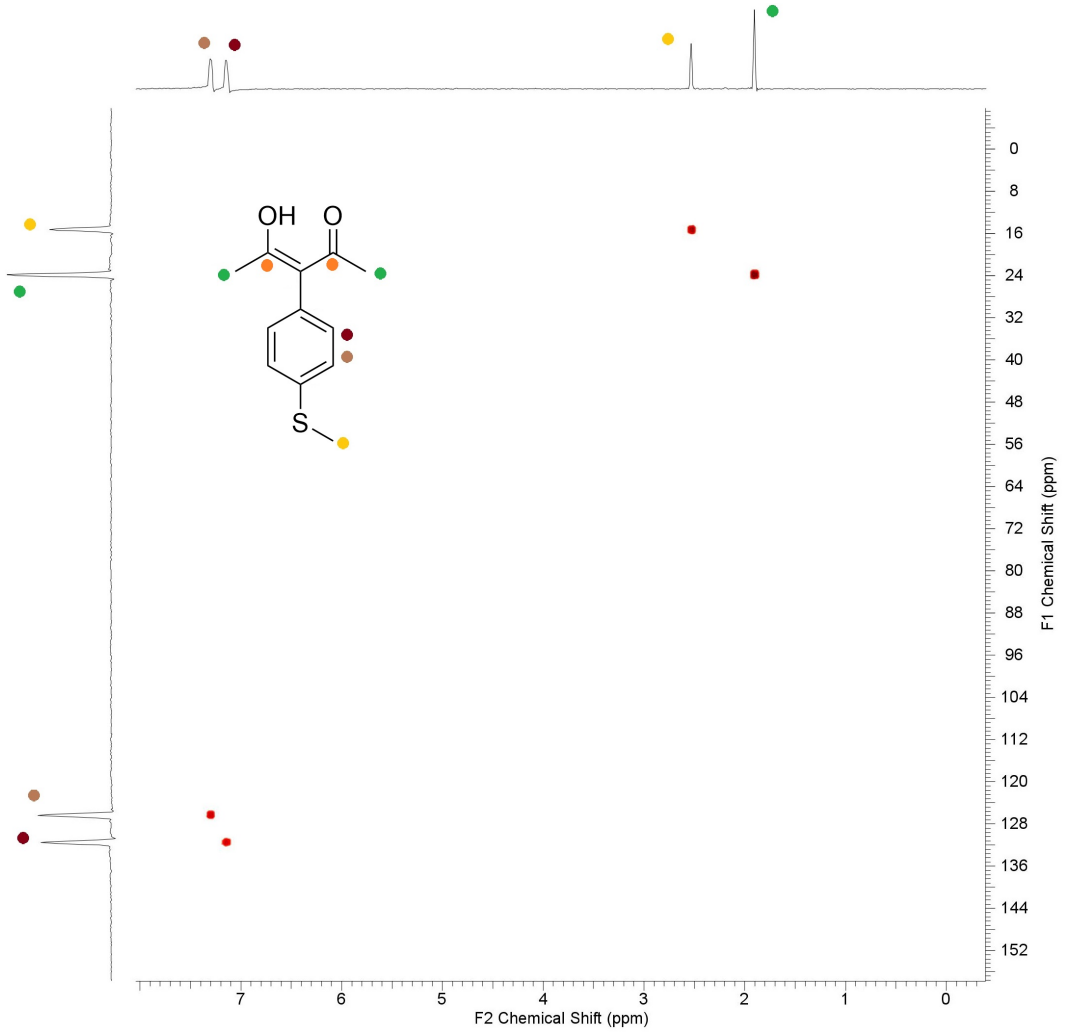

Fig. S19 HSQC spectrum of **5**. Measured in CD_2Cl_2 at 298 K.

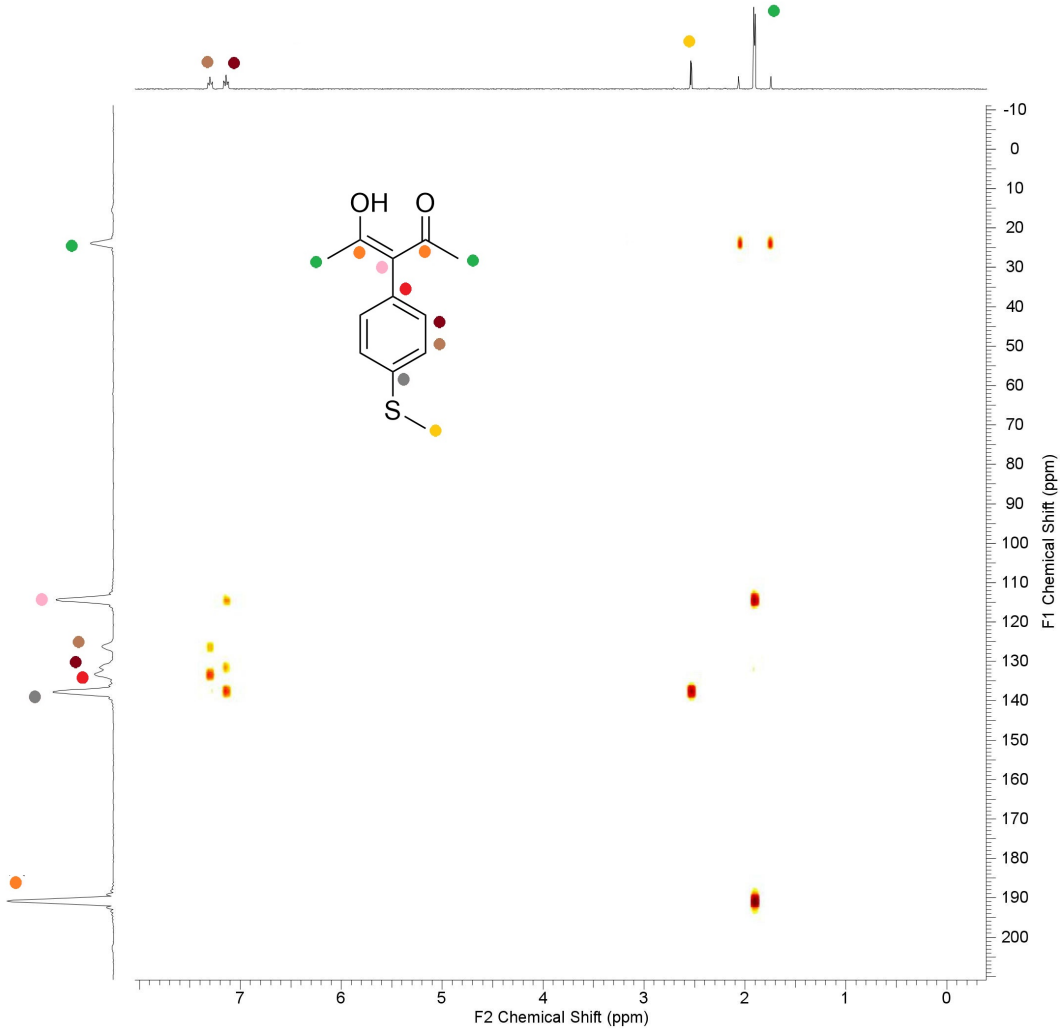

Fig. S20 HMBC spectrum of **5**. Measured in CD_2Cl_2 at 298 K.

S5 Crystal data

Table S5 Crystal data for **4**, **5**, **6a**, **7e** and **8a**.

Compound	**4**	**5**	**6a**	**7e**	**8a**
Empirical formula	$C_{13}H_{18}O_3S$	$C_{12}H_{14}O_2S$	$C_{36}H_{39}CoO_6S_3$	$C_{37.77}H_{42.54}GaO_{6.59}S_3$	$C_{38}H_{41}AgCl_7CoO_{10}S_3$
Moiety formula	$C_{13}H_{18}O_3S$	$C_{12}H_{14}O_2S$	$C_{36}H_{39}CoO_6S_3$	$C_{36}H_{39}GaO_6S_3$, 0.59 (C_3H_6O)	$C_{36}H_{39}AgClCoO_{10}S_3$, 2 ($CHCl_3$)
M_r / g mol^{-1}	254.33	222.29	722.78	767.84	1168.84
T / K	100(2)	100(2)	100(2)	100(2)	100(2)
Crystal description	colourless block	colourless block	green plate	orange block	green needle
Crystal size / mm^3	$0.39\times0.130\times0.10$	$0.22\times0.21\times0.15$	$0.27\times0.24\times0.07$	$0.31\times0.25\times0.13$	$0.49\times0.10\times0.05$
Crystal system	monoclinic	monoclinic	tetragonal	monoclinic	monoclinic
Space group (No.)	$P2_1/n$ (14)	$P2_1/c$ (14)	$I4_1/a$ (88)	$P2_1/c$ (14)	$P2_1/c$ (14)
a / Å	10.030(3)	11.096(3)	17.703(4)	14.603(4)	7.6747(9)
b / Å	10.614(4)	7.867(2)	17.703(4)	25.521(7)	31.666(4)
c / Å	13.284(4)	12.803(3)	46.013(8)	20.434(6)	18.994(3)
β / °	110.839(5)	92.821(4)	90	100.830(4)	96.898(2)
V / Å^3	1321.7(8)	1116.3(5)	14420(7)	7480(4)	4582.7(11)
Z	4	4	16	8	4
μ / mm^{-1}	0.239	0.266	0.692	0.949	1.388
Total/unique reflections	19581/3923	15713/2952	80739/6620	91300/15896	70088/13620
R_{int}	0.0359	0.0323	0.1027	0.1455	0.0809
$(\sin(\theta)/\lambda)_{max}$	0.72	0.68	0.60	0.63	0.72
Completeness to θ_{max}	0.967	0.997	1.000	0.995	0.972
$R\left[F^2>2\sigma(F^2)\right]$	0.0345	0.0368	0.0522	0.0678	0.0474
w$R_2(F^2)$	0.1019	0.0984	0.1279	0.1733	0.1236
GOF	1.098	1.029	1.078	1.014	1.053
No. of parameters	161	139	424	918	148
No. of restraints	0	0	0	2	0
$(\Delta\rho_{max}/\Delta\rho_{min})$ / e Å^{-3}	0.481/−0.279	0.397/−0.194	0.527/−0.538	0.739/−0.817	0.302/−0.234
CSD number	1968730	1968731	1968732	1968733	1968734

Table S6 Crystal data for **8b**, **8c**, **8d**, **8e** and **8f**.

Compound	**8b**	**8c**	**8d**	**8e**	**8f**
Empirical formula	$C_{38}H_{41}AgAlCl_7O_{10}S_3$	$C_{38}H_{41}AgCl_7CrO_{10}S_3$	$C_{38}H_{41}AgFeCl_7O_{10}S_3$	$C_{38}H_{41}AgGaCl_7O_{10}S_3$	$C_{38}H_{41}AgAl_{0.55}Cl_7Ga_{0.45}O_{10}S_3$
Moiety formula	$C_{36}H_{39}AgAlClO_{10}S_3$, $2(CHCl_3)$	$C_{36}H_{39}AgCrClO_{10}S_3$, $2(CHCl_3)$	$C_{36}H_{39}AgFeClO_{10}S_3$, $2(CHCl_3)$	$C_{36}H_{39}AgGaClO_{10}S_3$, $2(CHCl_3)$	$C_{36}H_{39}AgAl_{0.55}ClGa_{0.45}O_{10}S_3$, $2(CHCl_3)$
M_r / g mol^{-1}	1136.89	1161.91	1165.76	1179.63	1156.01
T / K	100(2)	100(2)	100(2)	100(2)	100(2)
Crystal description	colourless needle	purple block	red rod	colourless rod	colourless block
Crystal size / mm^3	$0.37 \times 0.09 \times 0.07$	$0.33 \times 0.12 \times 0.08$	$0.50 \times 0.09 \times 0.09$	$0.42 \times 0.10 \times 0.08$	$0.18 \times 0.17 \times 0.10$
Crystal system	monoclinic	monoclinic	monoclinic	monoclinic	monoclinic
Space group (No.)	$P2_1/c$ (14)	$P2_1/c$ (14)	$P2_1/c$ (14)	$P2_1/c$ (14)	$P2_1/c$ (14)
a / Å	7.6805(7)	7.6885(14)	7.674(3)	7.6796(17)	7.6934(9)
b / Å	31.867(3)	31.944(6)	32.075(13)	31.828(7)	31.866(4)
c / Å	19.0168(18)	19.105(4)	19.065(8)	19.013(5)	19.046(3)
β / °	97.514(2)	97.544(3)	97.790(7)	97.932(4)	97.751(2)
V / Å^3	4614.4(7)	4651.7(15)	4649(3)	4602.8(19)	4626.6(11)
Z	4	4	4	4	4
μ / mm^{-1}	1.05	1.244	1.323	1.607	1.294
Total/unique reflections	69783/13106	64891/11607	43264/8823	58880/10207	68006/12305
R_{int}	0.1159	0.1426		0.0969	0.1195
$(\sin(\theta)/\lambda)_{max}$	0.70	0.67	0.61	0.64	0.64
Completeness to θ_{max}	0.996	0.995	0.993	0.988	0.999
$R\left[F^2 > 2\sigma(F^2)\right]$	0.0511	0.0515	0.0654	0.0536	0.0394
$wR_2(F^2)$	0.1210	0.1232	0.1486	0.1234	0.0859
GOF	1.030	0.1038	1.077	1.110	0.98
No. of parameters	550	550	551	550	551
No. of restraints		0	0	0	0
$(\Delta\rho_{max}/\Delta\rho_{min})$ / e Å^{-3}	1.717/−0.924	0.988/−0.925	1.118/−0.947	0.988/−0.682	0.648/−0.598
CSD number	1968735	1968736	1968737	1968738	1968739

References

1 Bruker, *SAINT+: Program for Reduction of Data Collected on Bruker CCD Area Detector Diffractometer*, 2009.

2 Bruker, *SADABS*, 2008.

3 G. M. Sheldrick, *Acta Crystallogr., Sect. A: Found. Crystallogr.*, 2015, **71**, 3–8.

4 A. L. Spek, *Acta Crystallogr., Sect. C: Cryst. Struct. Commun.*, 2015, **71**, 9–18.

5 D. R. Allan, S. J. Clark, R. M. Ibberson, S. Parsons, C. R. Pulham and L. Sawyer, *Chem. Commun.*, 1999, 751–752.

6 H. Kroll, T. Lueder, H. Schlenz, A. Kirfel and T. Vad, *Eur. J. Mineral.*, 1997, **9**, 705–733.